

# Production of super selective polysulfone hollow fiber membranes for gas separation

A.F. Ismail<sup>a</sup>, I.R. Dunkin<sup>b</sup>, S.L. Gallivan<sup>b</sup>, S.J. Shilton<sup>c,\*</sup>

<sup>a</sup>Faculty of Chemical and Natural Resources Engineering, Universiti Teknologi Malaysia, P.O. Box 791, Sekudai 80990, Johor, Malaysia

<sup>b</sup>Department of Pure and Applied Chemistry, University of Strathclyde, Thomas Graham Building, 295 Cathedral Street, Glasgow G1 1XL, Scotland, UK

<sup>c</sup>Department of Chemical and Process Engineering, University of Strathclyde, James Weir Building, 75 Montrose Street, Glasgow G1 1XJ, Scotland, UK

Received 2 October 1998; received in revised form 8 December 1998; accepted 8 December 1998

## Abstract

Polysulfone gas separation hollow fiber membranes were manufactured using a dry/wet spinning process with forced convection in the dry gap. Hollow fibers were produced using two different bore coagulants: one pure water and one with reduced water activity. An optimized multi-component dope was used which proved to be a shear-thinning power-law fluid. For each bore system, membranes were spun at low and high dope extrusion rates (DERs) corresponding to shear rates of around  $4000\text{ s}^{-1}$  and  $10\,000\text{ s}^{-1}$ , respectively, at the outer spinneret wall. Plane polarized infrared spectroscopy was used to probe the membrane active layer. Pressure-normalized fluxes and selectivities were evaluated using pure carbon dioxide and methane. For the spinning conditions used here, the combination of reduced water activity in the bore and high DER produced highly selective membranes. Some selectivities reached about three times the recognized intrinsic value for the polymer. © 1999 Elsevier Science Ltd. All rights reserved.

**Keywords:** Hollow fiber membranes; Gas separation; Super selectivity

## Nomenclature

$P$	pressure-normalized flux, $\text{cm}^3$ (STP)/ ( $\text{s cm}^2\text{ cm Hg}$ )
$R_0$	reflected beam intensity of the reference
$R$	reflected beam intensity of the sample

## Greek letters

$\dot{\gamma}$	shear rate, $\text{s}^{-1}$
$\tau$	shear stress, Pa

## 1. Introduction

Research is ongoing to enhance the pressure-normalized flux and selectivity of asymmetric polymeric gas separation membranes. A thin and effectively undamaged active layer is required and a number of fabrication techniques, which control the conditions of phase inversion in various ways, have been employed to achieve this [1–3].

It is now possible to heighten membrane selectivity beyond the generally recognized intrinsic value for the

amorphous polymer [4–6]. This has been accomplished in a number of different ways for various polymers: polysulfone [7–10], polyethersulfone [11], polyestercarbonate [12], polyimide [13], polyamide [14] and cellulose acetate [15].

It has also been recognized that molecular orientation will affect membrane selectivity [5,12] and that orientation can be brought about by altering the rheological conditions during fabrication [16]. Shear and elongation during spinning have been shown to affect the permeation performance of polysulfone hollow fiber membranes [17,18] and this was attributed to molecular orientation in the active layer.

Molecular orientation in membranes can now be directly measured by spectroscopic techniques [19]. Plane polarized infrared spectroscopy has been used recently to confirm the presence of shear rate induced orientation in gas separation membranes [9,20]. For polysulfone hollow fibers, increased dope extrusion rate (DER) was shown to elevate membrane selectivity beyond the intrinsic value of the polymer [9,21].

Altering the internal coagulant system has also been shown to improve the gas separation performance of hollow fiber membranes [11,22]. It is thought that the integrity of the outer skin layer is compromised if solvent migration into the bore is too rapid [3]. A reduction in coagulant water

\*Corresponding author. Tel.: + 44-141-552-4400 ext. 2380; fax: 0141-552-2302.

E-mail address: simon.shilton@strath.ac.uk (S.J. Shilton)

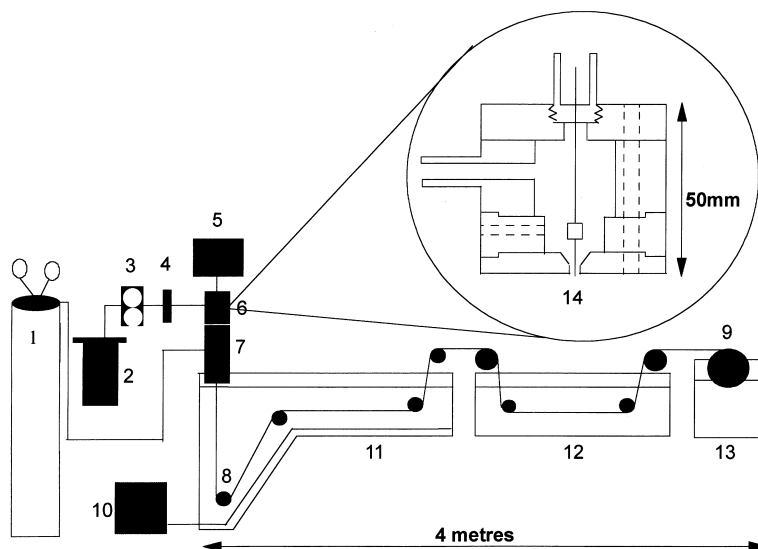


Fig. 1. Hollow fiber membrane spinning apparatus: (1) nitrogen; (2) dope reservoir; (3) gear pump; (4) filter, 7  $\mu\text{m}$ ; (5) syringe pump; (6) spinneret; (7) forced convection tube; (8) roller; (9) wind-up drum; (10) refrigeration/heating unit; (11) coagulation bath; (12) washing/treatment bath; (13) wind-up bath; (14) schematic of a spinneret.

activity in the bore slows down inward solvent diffusion which protects the active layer from perforation.

This paper investigates the effects of increased shear during spinning and decreased coagulant water activity in the bore fluid with a view to producing highly selective polysulfone hollow fiber membranes. A unique dry/wet spinning system was used with a particular forced convection setup in the dry gap. The specific details of the process are given in this paper. The forced convection approach, in general, is one means of producing non-porous active layers in polymeric membranes [23].

Molecular orientation in the membrane active layer was investigated using plane polarized infrared spectroscopy, a technique that has been employed in other fiber applications [24].

## 2. Experimental

### 2.1. Membrane spinning

Asymmetric polysulfone hollow fiber membranes for gas separation were fabricated using a dry/wet spinning process with forced convection in the dry gap (Fig. 1). An optimized four component dope was used [7]: 22% (w/w) polysulfone, 31.8% (w/w) *N,N* dimethylacetamide, 31.8% (w/w) tetrahydrofuran and 14.4% (w/w) ethanol. The dope reservoir was at ambient temperature ( $20^\circ\text{C} \pm 2^\circ\text{C}$ ) during spinning. On extrusion from the spinneret (spinneret dimensions: OD 600  $\mu\text{m}$ /ID 330  $\mu\text{m}$ ), the fiber passed through a cylindrical forced convection chamber (length 9 cm, diameter 5 cm) which was flushed with 4  $\text{l min}^{-1}$  of nitrogen gas. The nitrogen was introduced through a 1/4 in. tube which abutted upon the chamber normal to the surface at mid-height. A

2 mm clearance existed between the top of the forced convection chamber and the bottom plate of the spinneret and also between the bottom of the forced convection chamber and the water level in the first coagulation bath.

Pure water at  $14^\circ\text{C} \pm 0.5^\circ\text{C}$  was used in the external coagulation baths. The bore coagulant was either pure water or a 20% (w/w) solution of potassium acetate in water at ambient temperature. This equates to water activities of 1 and 0.9 [3] respectively. At both bore water activities, hollow fibers were spun at two DERs and hence at different levels of shear. The stretch ratio (wind up speed/extrusion speed) was fixed at 1 throughout. The ratio of DER to bore fluid injection rate was also kept constant at a value of 3. After spinning, the membranes were steeped in water and then dried using a methanol solvent exchange technique [25].

### 2.2. Gas permeation

The pressure-normalized fluxes of the fibers were measured for pure carbon dioxide and methane at  $25^\circ\text{C}$  and at a pressure drop of 5 bar. The membranes were also tested after coating with silicone (Sylgard 184, Dow Corning); a standard technique that repairs any imperfections or pores that appear in the active layer [26]. Membrane selectivities were determined by taking the ratio of the pressure-normalized fluxes.

### 2.3. Plane polarized IR spectroscopy

Molecular orientation in the active layer of the membranes was directly measured using plane polarized reflectance infrared spectroscopy. This technique can reveal anisotropy on the molecular level within a sample. Pronounced infrared dichroism (the difference in absorption

Table 1  
Effect of shear rate on gas permeation properties of polysulfone hollow fiber membranes-pure water in the bore<sup>a</sup>

Module	Uncoated		Coated	
	( $P_{\text{CO}_2}$ )	( $P_{\text{CO}_2}/P_{\text{CH}_4}$ )	( $P_{\text{CO}_2}$ )	( $P_{\text{CO}_2}/P_{\text{CH}_4}$ )
DER = 1.0 cm <sup>3</sup> min <sup>-1</sup> (low shear)				
L1	69.4	1.30	35.4	7.07
L2	67.0	1.35	39.5	7.70
L3	45.1	1.83	33.5	4.46
L4	45.8	2.93	24.2	5.73
L5	49.4	1.30	32.1	5.97
L6	43.7	1.22	23.7	4.47
L7	37.8	2.05	28.3	5.44
L8	65.2	1.39	68.7	7.81
DER = 2.5 cm <sup>3</sup> min <sup>-1</sup> (high shear)				
H1	64.2	1.71	47.5	32.1
H2	80.7	1.63	38.1	40.2
H3	88.2	2.18	54.7	13.9
H4	76.5	2.65	50.5	30.1
H5	81.3	2.64	50.2	32.7
H6	79.8	2.31	43.0	34.3
H7	54.8	3.69	48.8	13.6
H8	57.5	4.15	51.3	22.3
H9	62.5	3.50	58.1	41.5

<sup>a</sup> Here  $P$  is the pressure-normalized flux  $\times 10^6$  (cm<sup>3</sup> (STP)/(s cm<sup>2</sup> cm Hg)), measured at 25°C and at a pressure differential of 5 bar.

between parallel and perpendicularly polarized light) indicates anisotropy, while the absence of dichroism shows that a sample has random orientation.

The IR spectra were recorded on a Bomem MB-100 Fourier transform IR spectrometer with a modified top plate. With this arrangement, the beam from the interferometer was focused at a point about 2.5 cm outside the instrument

Table 2  
Effect of shear rate on gas permeation properties of polysulfone hollow fiber membranes-reduced water activity in the bore<sup>a</sup>

Module	Uncoated		Coated	
	( $P_{\text{CO}_2}$ )	( $P_{\text{CO}_2}/P_{\text{CH}_4}$ )	( $P_{\text{CO}_2}$ )	( $P_{\text{CO}_2}/P_{\text{CH}_4}$ )
DER = 1.0 cm <sup>3</sup> min <sup>-1</sup> (low shear)				
LA1	17.6	6.45	14.3	41.1
LA2	17.0	9.70	16.4	34.9
LA3	17.9	2.91	14.4	46.5
LA4	18.4	3.65	13.7	37.5
LA5	17.7	4.82	14.4	33.1
LA6	16.8	5.51	14.6	46.7
LA7	120	1.54	35.7	33.6
DER = 2.5 cm <sup>3</sup> min <sup>-1</sup> (high shear)				
HA1	30.5	2.94	32.6	70.0
HA2	58.2	3.11	33.4	73.0
HA3	34.2	6.13	20.8	54.4
HA4	62.1	2.15	22.8	41.6
HA5	72.6	1.91	35.3	82.8
HA6	102	1.62	38.5	83.1
HA7	85.6	1.73	43.4	54.0

<sup>a</sup> Here  $P$  is the pressure-normalized flux  $\times 10^6$  (cm<sup>3</sup> (STP)/(s cm<sup>2</sup> cm Hg)), measured at 25°C and at a pressure differential of 5 bar.

case and the detector was located so as to collect reflected radiation from a sample placed at or near this focus. The results reported here were all obtained with an MCT detector at a resolution of 4 cm<sup>-1</sup>. The spectrometer was interfaced via a DSP-100 fast Fourier transform card to a Viglen 25 MHz 386SX computer with a co-processor. Spectra were acquired either with standard Bomem software or with Galactic Industries LabCalc. The use of this spectrometer to examine low-temperature matrices has been described previously [27].

The IR beam of the spectrometer was polarized with a SpecAc aluminum grid polarizer on a KRS-5 substrate held in a rotatable mount. The polarizer was located in the incident beam to avoid any optical components between the polarizer and sample. Spectra could be recorded with the plane of polarization at any angle to the vertical, but best results were obtained when this plane was maintained vertical and the sample itself was rotated. Experiments with the polarizer at various angles revealed that there was little or no intrinsic instrument polarization.

Spectra of the hollow fiber membranes were obtained from samples wound around a rectangular KBr plate. The plate was mounted vertically at the sample position with the fibers running either vertically or horizontally. Thus for each sample, the IR spectra were obtained with the plane of polarization parallel and perpendicular to the shear direction. Reference spectra were recorded using the blank KBr plate.

#### 2.4. Spinning dope rheology and flow profile in spinnerets

Rheological tests were carried out at 20°C using a Carri-Med Rheometer. The spinning dope was subjected to a range of shear rates (consistent with fiber extrusion) and the corresponding shear stresses were recorded.

The flow profile in the spinneret was established by solving the flow equations for a power-law fluid in a concentric annulus [28].

### 3. Results

#### 3.1. Gas permeation

The effect of DER on gas permeation properties is shown in Tables 1 and 2 for fibers spun with pure water and reduced water activity in the bore, respectively. Numerous modules were tested to check reproducibility. Uncoated membranes exhibit relatively low selectivities suggesting the presence of surface pores or imperfections. Coated results are more relevant as they represent membrane performance. It can be seen that in both bore systems, an increase in DER results in an increase in selectivity. The results also show that three out of the four membrane categories exhibit selectivities that exceed the recognized polysulfone intrinsic selectivity of 30 [11].

However, the data for the high extrusion rate fibers spun

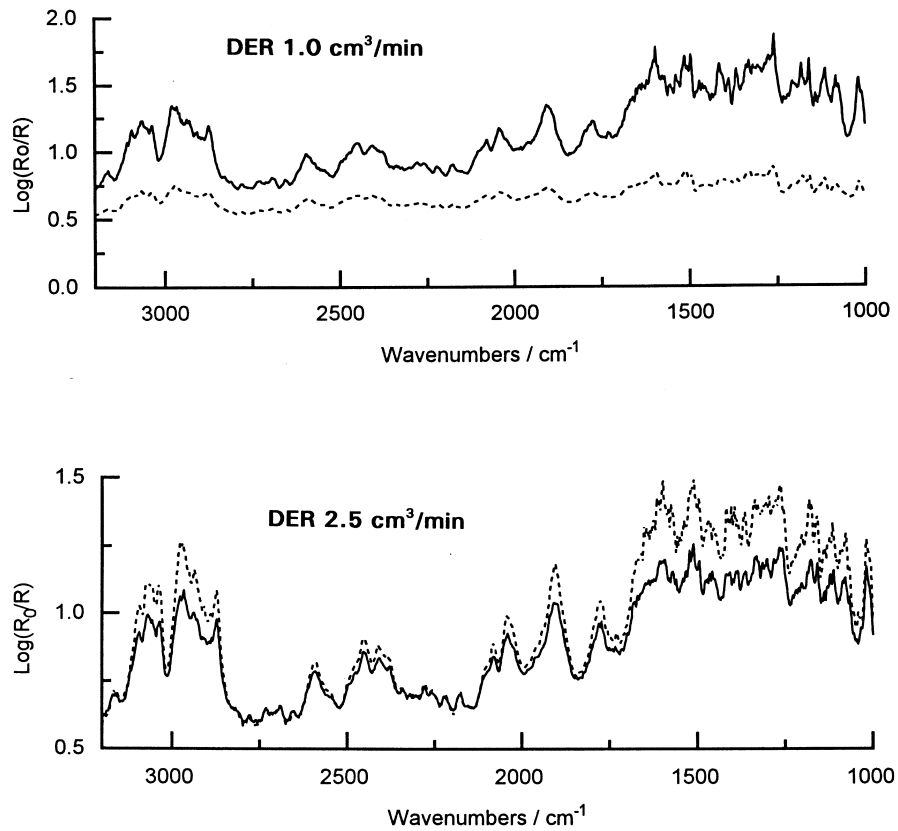


Fig. 2. Polarized reflection IR spectra of the low-shear (upper traces) and the high-shear (lower traces) hollow fiber membranes spun with reduced water activity in the bore. The solid lines represent spectra taken with polarization parallel to the fiber axis i.e. parallel to the shear direction. The dashed lines represent spectra taken with polarizations perpendicular to the fiber axis.  $R_o/R$  is the ratio of the reflected beam intensities of the reference and the sample.

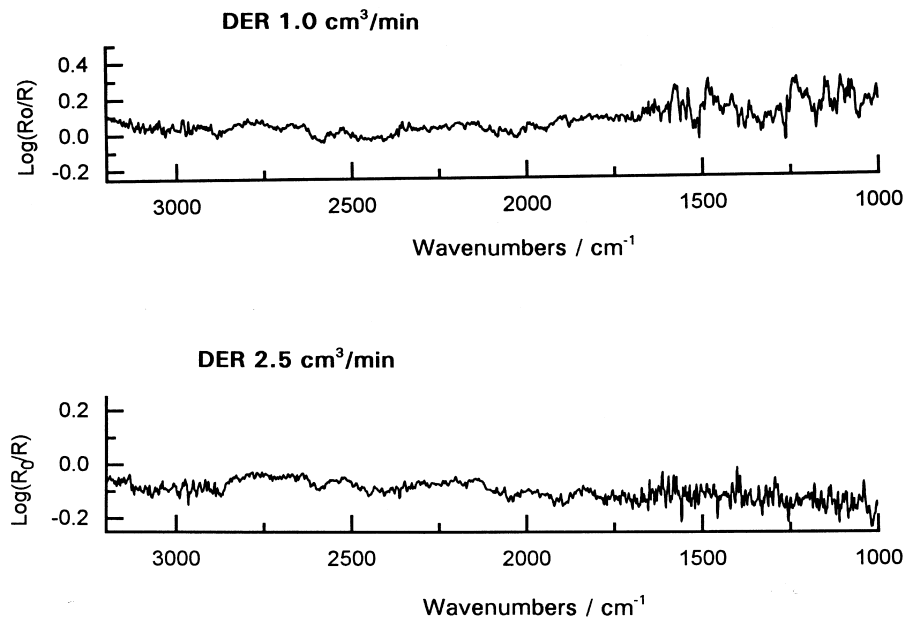


Fig. 3. Normalized difference spectra (parallel–perpendicular) of the low-shear (upper trace) and the high-shear (lower trace) hollow fiber membranes spun with a reduced water activity in the bore.  $R_o/R$  is the ratio of the reflected beam intensities of the reference and the sample.

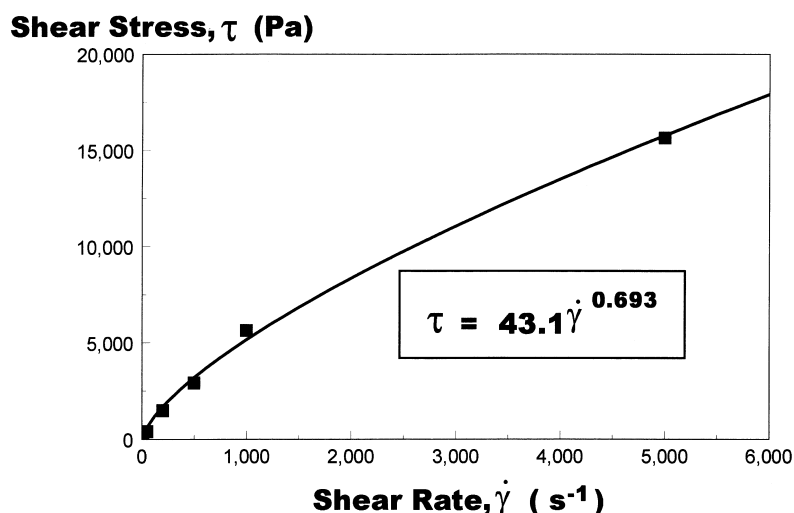


Fig. 4. Flow curve for the spinning dope (22% (w/w) polysulfone, 31.8% (w/w) *N,N* dimethylacetamide, 31.8% (w/w) tetrahydrofuran and 14.4% (w/w) ethanol).

with reduced water activity in the bore are particularly striking (Table 2): selectivities reach up to almost three times the intrinsic value for the polymer.

### 3.2. Plane polarized IR spectroscopy

Fig. 2 shows polarized reflection IR spectra for both low and high extrusion rate fibers spun with reduced water activity in the bore. Anisotropy in both fiber types is apparent by the difference in intensity of reflection between the parallel and perpendicularly polarized spectra. The difference for the low extrusion rate membranes is interesting, showing a significant reduction in absorption in perpendicular compared to parallel polarization.

Fig. 3 shows the difference spectra obtained after normalization on the prominent isolated IR band at  $1905\text{ cm}^{-1}$ . After normalization, the spectra in different polarizations

are similar and the difference spectra show few prominent features. It is therefore difficult to comment on molecular orientation.

These observations contrast with the IR spectra obtained for the fibers spun with pure water in the bore which have already been reported [9]. The difference spectra for these membranes showed clear distinctions indicative of increased molecular orientation at high shear. Previous IR spectra obtained for flat sheet membranes have also demonstrated shear induced molecular orientation [20].

### 3.3. Spinning dope rheology and flow profile in spinnerets

The flow curve for the spinning dope is given in Fig. 4. As can be seen, the dope behaves as a shear-thinning power law fluid (index 0.693, constant  $43.1\text{ (Pa s}^n)$ ).

Fig. 5 shows the shear rate profiles in the spinneret for

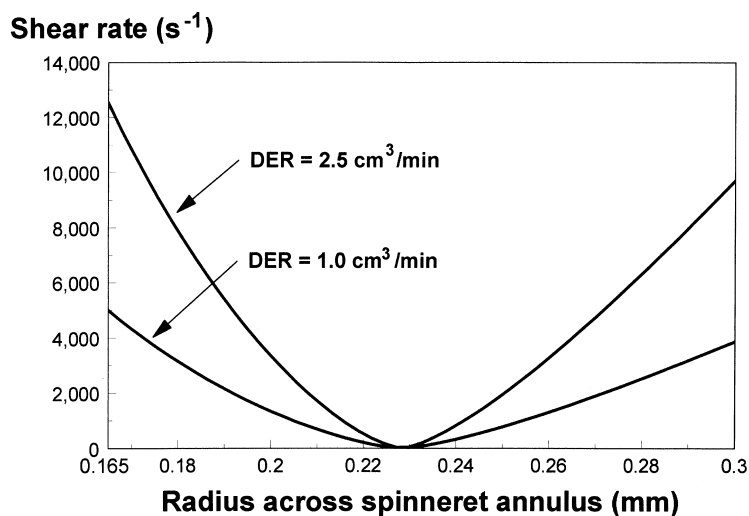


Fig. 5. Shear rate profiles in spinneret at low and high extrusion rates.

low and high DERs. The main interest is the level of shear experienced at the spinneret wall. As a result of the forced convection in the dry gap, the coagulation of the outermost region of the fiber is effectively instantaneous on emergence from the spinneret. Therefore, the shear rate induced at the spinneret wall affects the structure of the membrane active layer.

#### 4. Discussion

The performance of gas separation hollow fiber membranes depends on many factors. Fabrication conditions, whether rheological or those relating to phase inversion, determine membrane structure which in turn controls pressure-normalized flux and selectivity.

Tables 1 and 2 suggest a number of trends. The pressure-normalized flux increases with increasing DER for both bore coagulants. This is consistent with a decrease in active layer thickness with increasing DER<sup>1</sup> which may relate to the corresponding decrease in the dry gap residence time. Skin coalescence and growth occur over a shorter period of time in the forced convection chamber for high DER fibers possibly resulting in the establishment of a thinner active layer prior to wet phase inversion. (DER 1 cm<sup>3</sup> min<sup>-1</sup> – residence time 1.1 s, DER 2.5 cm<sup>3</sup> min<sup>-1</sup> – residence time 0.43 s.)

At either DER, the reduced water activity fibers have lower pressure-normalized fluxes. This suggests that lowering the water activity of the bore fluid tends to produce thicker skins<sup>2</sup>.

The dope solution used in this work was shear thinning (Fig. 4) suggesting that as the shear rate is increased the polymer molecules become more aligned. It is generally accepted that under shear flow, polymer molecules tend to orient themselves in the flow direction [29–32]. Viscoelasticity theory [33] explains this in terms of stretching polymer chains between entanglement junctions [34]. However, other mechanisms have been proposed such as those of Paul [29] and Serkov and Khanchic [35].

During fiber extrusion, the highest shear rates occur at the spinneret wall and increase with increasing DER (Fig. 5). It seems reasonable to suggest that molecular orientation is ‘frozen’ into the active layer of the membrane in the forced convection chamber where the onset of solidification in the outermost regions of the fiber will be effectively instantaneous. The multi-component dope was designed to achieve the rapid solidification of a non-porous membrane active layer under forced convection conditions [3,7,23]. The

presence of the non-solvent, ethanol, in the dope brings the system nearer to thermodynamic instability. The tetrahydrofuran solvent in the dope is highly volatile and is rapidly driven off under forced convection conditions. The result is effectively immediate phase inversion. The polymer rich regions are forced to coalesce by capillary pressures [23] and the polymer rich phase undergoes rapid vitrification thus producing an oriented membrane skin with few pores or defects. (*N,N* dimethylacetamide is the base solvent.)

It is proposed that an increase in DER, and hence an increase in shear rate, will enhance molecular orientation in the fiber skin which will in turn boost membrane selectivity. Tables 1 and 2 show an increase in selectivity with increasing DER but direct evidence of increased molecular alignment with increasing DER can only be sought in the spectroscopic results.

Anisotropy is clearly evident in the IR spectroscopy for the reduced water activity fibers (Fig. 2). This shows that direction dependent structural differences occur when shear is increased but the lack of detail in the difference spectra (Fig. 3) precludes any strong comment on molecular orientation. It is unfortunate that the spectra were not more conclusive. Traces of potassium acetate, if they were to exist in the membrane wall, may mask molecular orientation by causing de-polarization. However, the difference spectra for the fibers spun with pure water in the bore, reported earlier [9], did show clear distinctions indicative of increased molecular orientation at high shear.

In addition, the membranes have recently been tested using positron annihilation lifetime spectroscopy (PALS) to further investigate the conformation of the active layer at the molecular level. The results are only briefly mentioned here but will be reported and discussed fully in a forthcoming paper [36]. The tests indicate that as DER is increased the number of free volume cavities in the active layer increases for both bore systems. This may relate to an increase in molecular orientation at higher shear. An increase in the number of cavities concurs with the observed rise in pressure-normalized flux and selectivity with increasing DER (Tables 1 and 2). The mean free volume cavity diameter was found to be consistent across all membrane types at a value of 5.4 Å. This cavity size may act as a gate to the CO<sub>2</sub> and hence pressure-normalized flux and selectivity rise with increasing DER owing to the increase in the number of gates.

The number of free volume cavities in the reduced water activity fibers was found to be greater than in the pure water fibers regardless of DER. This could explain the greater selectivities of the reduced water activity fibers generally.

The coincidence of a mean cavity diameter of 5.4 Å and the highest number of cavities in the highly selective membranes (high DER, low bore water activity) is interesting. Chen et al [15] also experienced extremely high selectivities (values of over 200 for CO<sub>2</sub>/CH<sub>4</sub> in cellulose acetate membranes) and they rationalised this by postulating a pore

<sup>1</sup> Although micrographs are not included here because of photographic difficulties, scanning electron microscopy supported this. For both bore systems, an increase in DER resulted in a switch from a thicker active layer and sponge-like substructure to a thinner active layer and macroporous substructure.

<sup>2</sup> Again, scanning electron microscopy supported this. At a fixed DER, active layers were thicker in reduced water activity fibers.

Table 3  
O<sub>2</sub>/N<sub>2</sub> permeation data (effect of bore coagulant and shear rate)<sup>a</sup>

Uncoated		Coated	
(P <sub>O<sub>2</sub></sub> )	(P <sub>O<sub>2</sub></sub> /P <sub>N<sub>2</sub></sub> )	(P <sub>O<sub>2</sub></sub> )	(P <sub>O<sub>2</sub></sub> /P <sub>N<sub>2</sub></sub> )
Pure water in the bore			
DER = 1.0 cm <sup>3</sup> min <sup>-1</sup> (low shear)			
6.06	1.44	7.96	1.72
DER = 2.5 cm <sup>3</sup> min <sup>-1</sup> (high shear)			
25.5	1.14	5.56	4.90
Reduced water activity in the bore			
DER = 1.0 cm <sup>3</sup> min <sup>-1</sup> (low shear)			
3.94	2.72	2.51	6.41
DER = 2.5 cm <sup>3</sup> min <sup>-1</sup> (high shear)			
29.3	1.11	6.91	7.32

<sup>a</sup> Here *P* is the pressure-normalized flux × 10<sup>6</sup> (cm<sup>3</sup> (STP)/(s cm<sup>2</sup> cm Hg)), measured at 25°C and at a pressure differential of 5 bar.

flow mechanism relating to the same level of cavity size as that found in this work. The kinetic diameter of CO<sub>2</sub> is 3.3 Å compared to 3.8 Å for CH<sub>4</sub>. The pore flow mechanism is a form of ‘molecular sieving’ and may be a possible explanation as to why a membrane with a mean cavity diameter of 5.4 Å and a high number of cavities is strongly discriminating between CO<sub>2</sub> and CH<sub>4</sub> beyond the realm of the solution diffusion mechanism.

In terms of the spinning system described here, the combination of a high extrusion rate with a reduced water activity in the bore produces highly selective polysulfone hollow fiber membranes. This may be because a highly engineered active layer is produced which delivers selectivities beyond those predicted by the solution diffusion mechanism. The dope used in this work was fairly dilute and the forced convection conditions somewhat aggressive. The convective gas (unhumidified nitrogen) was introduced into the convection chamber as a single jet which would have impinged on the hollow fiber at a single point before general dispersion. These conditions would encourage rapid solidification and effective skin formation. In the context of the skin formation theory postulated by Pinnau and Koros [23], coalescence of polymer rich nodules may be unusually smooth and efficient in this work as a relatively dilute dope would result in nodules with low rigidity moduli. Such special and instantaneous skin formation conditions may provide a platform for rheological manipulation of the active layer to produce molecular orientation and hence super selectivity in the resulting membrane. It would seem that lowering the bore fluid coagulation strength is necessary to preserve/protect the sophisticated conformation of a highly selective active layer.

The high extrusion rate low bore water activity fibers in this work also exhibit selectivities significantly above the intrinsic value for other gas systems. For a brief comparison, representative data for all membrane types are given in Table 3 for O<sub>2</sub>/N<sub>2</sub> [37] where the intrinsic selectivity is about 6.2 [38].

The industrial usefulness of the membranes in this work as a means of separating gases should be verified by gas mixture experiments. A variety of factors can make mixed gas separation results differ from those with only pure gases. Such tests are planned and will be reported in due course.

A full explanation of the results given in this paper would involve an in depth study of the underlying membrane formation mechanisms. Issues such as nodule formation and size, polymer molecule dimensions, the influence of shear fields on phase inversion [39] and rheologically induced polymer molecule orientation would need to be reconciled. A more thorough characterization of the conformation of the membrane active layer is also required to allow a better understanding of gas transmission properties.

## 5. Conclusions

For a forced-convection spinning process, the combination of a high extrusion rate (shear rate) and a reduced water activity in the bore produces highly selective polysulfone hollow fiber membranes. It is proposed that if special skin formation conditions prevail, increased shear can create an oriented and highly ordered membrane active layer which can exhibit selectivities significantly greater than the recognized intrinsic value for the isotropic polymer. It would seem that lowering the bore fluid coagulation strength is necessary to preserve a highly engineered super-selective active layer.

## References

- [1] Chung TS, Teoh SK, Hu X. *Journal of Membrane Science* 1997;133:161.
- [2] van't Hof JA, Reuvers AJ, Boom RM, Rolevink HHM, Smolders CA. *Journal of Membrane Science* 1992;70:17.
- [3] Pesek SC, Koros WJ. *Journal of Membrane Science* 1994;88:1.
- [4] Pinnau I, Koros WJ. *Journal of Applied Polymer Science* 1992;46:1195.
- [5] Pfromm PH, Pinnau I, Koros WJ. *Journal of Applied Polymer Science* 1993;48:2161.
- [6] Rezac ME, Le Roux JD, Chen H, Paul DR, Koros WJ. *Journal of Membrane Science* 1994;90:213.
- [7] Pesek SC, Koros WJ. *Journal of Membrane Science* 1993;81:71.
- [8] Ghosal K, Chern RT, Freeman BD, Daly WH, Negulescu II. *Macromolecules* 1996;29:4360.
- [9] Ismail AF, Shilton SJ, Dunkin IR, Gallivan SL. *Journal of Membrane Science* 1997;126:133.
- [10] Pinnau I, Koros WJ. *Journal of Membrane Science* 1992;71:81.
- [11] Li S-G, PhD Thesis, University of Twente, 1994.
- [12] Pinnau I, Hellums MW, Koros WJ. *Polymer* 1991;32:2612.
- [13] Kawakami H, Mikawa M, Nagaoka S. *Journal of Applied Polymer Science* 1996;62:965.
- [14] Mohammadi AT, Matsuura T, Sourirajan S. *Gas Separation and Purification* 1995;9:181.
- [15] Chen Y, Fouda AE, Matsuura T. In: *Advances in Reverse Osmosis and Ultrafiltration*, National Research Council of Canada, Vancouver, 1989. p. 259–278.
- [16] Puri PS. *Gas Separation and Purification* 1990;4:29.
- [17] Shilton SJ, Bell G, Ferguson J. *Polymer* 1994;35:5327.

- [18] Shilton SJ, Bell G, Ferguson J. *Polymer* 1996;37:485.
- [19] Khulbe KC, Gagné S, Tabe Mohammadi A, Matsuura T, Lamarche AM. *Journal of Membrane Science* 1995;98:201.
- [20] Shilton SJ, Ismail AF, Gough PJ, Dunkin IR, Gallivan SL. *Polymer* 1997;38:2215.
- [21] Ismail AF, Shilton SJ. *Journal of Membrane Science: Rapid Communication* 1998;139:285.
- [22] Chung TS, Kafchinski ER. *Journal of Applied Polymer Science* 1997;65:1555.
- [23] Pinnau I, Koros WJ. *Journal of Polymer Science: Part B: Polymer Physics* 1993;31:419.
- [24] Xue G. *Makromol. Chem.: Rapid Commun.* 1985;6:811.
- [25] Manos P. US Patent 4120098, 1978.
- [26] Ward RR, Chang RC, Danos JC, Carden JA. (Monsanto Co.) US Patent 4214020, 1980.
- [27] Dunkin IR, Gallivan SL. *Vibrational Spectroscopy* 1995;9:85.
- [28] Shilton SJ. *Journal of Applied Polymer Science* 1997;65:1359.
- [29] Paul DR. *Journal of Applied Polymer Science* 1969;13:817.
- [30] Mackley MR. *Journal of Polymer Science: Polymer Symposium* 1985;73:75.
- [31] Ferguson J, Doulgeris C, McKay GR. *Journal of Non-Newtonian Fluid Mechanics* 1980;6:333.
- [32] Ziabicki A. *Fundamentals of Fibre Formation*. New York: Wiley, 1976.
- [33] Ferry JD. *Viscoelastic Properties of Polymers*. New York: Wiley, 1980.
- [34] Graessley WW. *Journal of Chemical Physics* 1965;43:2696.
- [35] Serkov AT, Khanchich OA. *Khimicheskie Volokna* 1977;4:12.
- [36] Ismail AF, Hill AJ, Shilton SJ. In preparation.
- [37] Ismail AF, Sharpe ID, Dunlop GR, Shilton SJ. Unpublished work.
- [38] Pinnau I, Koros WJ. *Journal of Applied Polymer Science* 1991;43:1491.
- [39] Wolf BA. *Macromolecules* 1984;17:615.